

A COMPUTER SIMULATION STUDY OF THE MICROSCOPIC STRUCTURE OF A TYPICAL CURRENT SHEET IN THE SOLAR WIND

M. Roth
Institute for Space Aeronomy
3, Avenue Circulaire
B-1180 Brussels
Belgium

1. INTRODUCTION

Kinetic theories of tangential discontinuities (TD) in space plasmas have been discussed by a number of authors (e.g., Alpers, 1969; Roth, 1978; 1979; 1980; and 1983; Lee and Kan, 1979). These theories consider unidimensional plane current layers and the determination of their microscopic structure is based on both Vlasov and Maxwell's equations for plasma and fields. It is outside the scope of this paper to give a detailed account of these theories, but the interested reader can refer to Roth (1980, 1983) for the theoretical aspect sustaining the numerical results given in this note.

In section 2 we will give numerical results for the internal structure of a typical current sheet in the solar wind. Finally, the time resolution of plasma measurements across such a layer will be discussed in section 3 in the frame of a Interdisciplinary Study of Directional Discontinuities in the Solar Wind with the Ulysses Mission (Lemaire et al., 1983).

2. THE INTERNAL STRUCTURE OF A TYPICAL CURRENT SHEET

In a cartesian coordinate system, the plane of a tangential discontinuity is parallel to the (Y,Z) plane and all the variables are assumed to depend on the X coordinate, normal to the discontinuity.

Plasma boundary conditions for a typical current sheet in the solar wind are given in table I. On the left hand side of the transition, or side 1, i.e. for large negative values of X, there is a "hot" plasma of hydrogen and helium, while on the right hand side or side 2, i.e. for large positive values of X, there is a "cold" plasma of hydrogen and helium. Notice that on side 1, each plasma component has a distinct mean velocity. Note also that the "hot" plasma species have a vanishing number density on side 2 while the "cold" ones have a vanishing number density on side 1. The transition itself will be a region where these two plasmas of different characteristics are interpenetrated. The plasma in the transition will therefore

	N_1	N_2	T_1	T_2	V_{y1}	V_{y2}	V_{z1}	V_{z2}
e	5	3	15	10	219	175	-311	-285
H ⁺	4.5	2.7	6	4	223	175	-315	-285
He ⁺⁺	0.25	0.15	16	12	180	175	-272	-285
	cm ⁻³		eV		km/s		km/s	

Table I. The indices 1 and 2 refer respectively to sides 1 and 2, i.e., to large negative and large positive values of X .

be considered as a three-components plasma (e^- , H^+ and He^{++} , an admixture of the two adjacent plasmas. The magnetic field on side 1 is assumed to be uniform ($B_x = -B_y = 3.5$ nT). Its intensity on side 2 is, of course, predetermined from the pressure balance condition. On each side of the transition, the plasma boundary values satisfy the charge neutrality and the zero current density conditions.

The first three panels of figure 1 illustrate the number densities. The second panel displays the total number density of electrons (e^-), protons (H^+) and helium particles (He^{++}), i.e. the sum of the number densities of the cold and hot particles, illustrated on the first and third panels. Also in figure 1 are displayed the temperatures: 5th panel for the "hot" plasma species, 7th panel for the "cold" plasma species and 6th panel for the average temperatures of the admixture. Notice that the cold and hot electron temperatures do not change throughout the transition. This is a consequence of a particular choice for the parameters of the electron velocity distribution functions. Indeed, for the two electron species, it has been assumed that the velocity distribution functions remain isotropic about their mean velocity. Computation of the temperature (and also of moments of non-zero order) becomes meaningless, of course, when the corresponding number density becomes vanishingly small, as shown in the 5th and the 7th panels. Panels 4 and 8 of figure 1 illustrate, respectively, the y and z components of the energy flow in the admixture. The thickness of the transition in unit of the proton gyroradius, $R(H^+)$, can be deduced from the scale shown in the upper part of the panels. It can be seen that the variation in the H^+ number density occurs in about $20 R(H^+)$, i.e., in about 800 km.

The 12 panels of figure 2 illustrate the electric potential (1st panel), the electric field (5th panel), the relative charge density (9th panel), the current density components (2nd panel), the magnetic field components (6th panel) and hodogram (10th panel), the contribution of each plasma species to the current density (3rd, 4th, 7th and 8th panels) and to the plasma kinetic pressure (11th panel) and finally (12th panel) the pressure balance condition.

Figure 3 shows how each plasma species contributes to the bulk velocity of the plasma. Panels 1-2-3, 5-6-7 and 9-10-11 illustrate

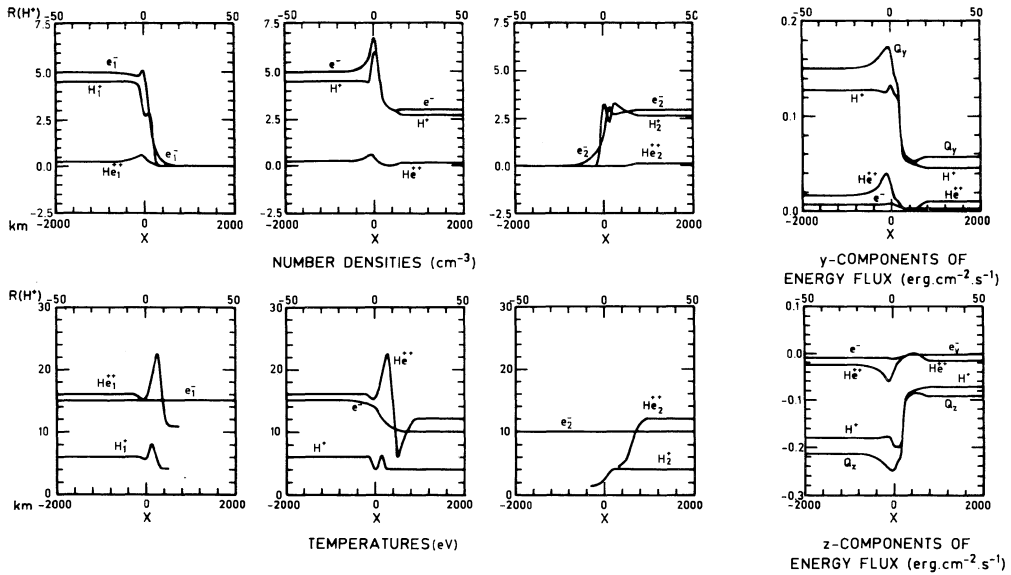


Figure 1. Plasma characteristics across a TD whose boundary conditions are given in table I.

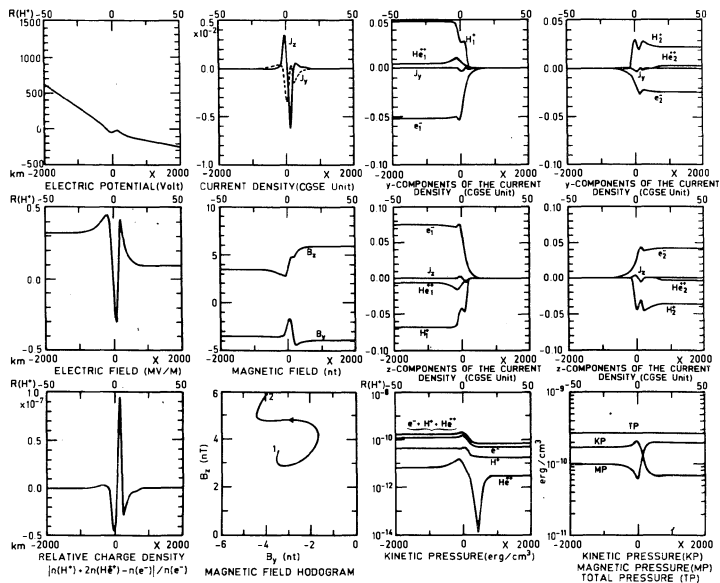


Figure 2. Fields and current characteristics across a TD whose boundary conditions are given in table I.

respectively the mean velocity of electron, proton and helium species. The hodograms illustrated in panels 8 and 12 show that the protons carry most of the bulk velocity of the plasma, as can also be seen from panels 4 and 6.

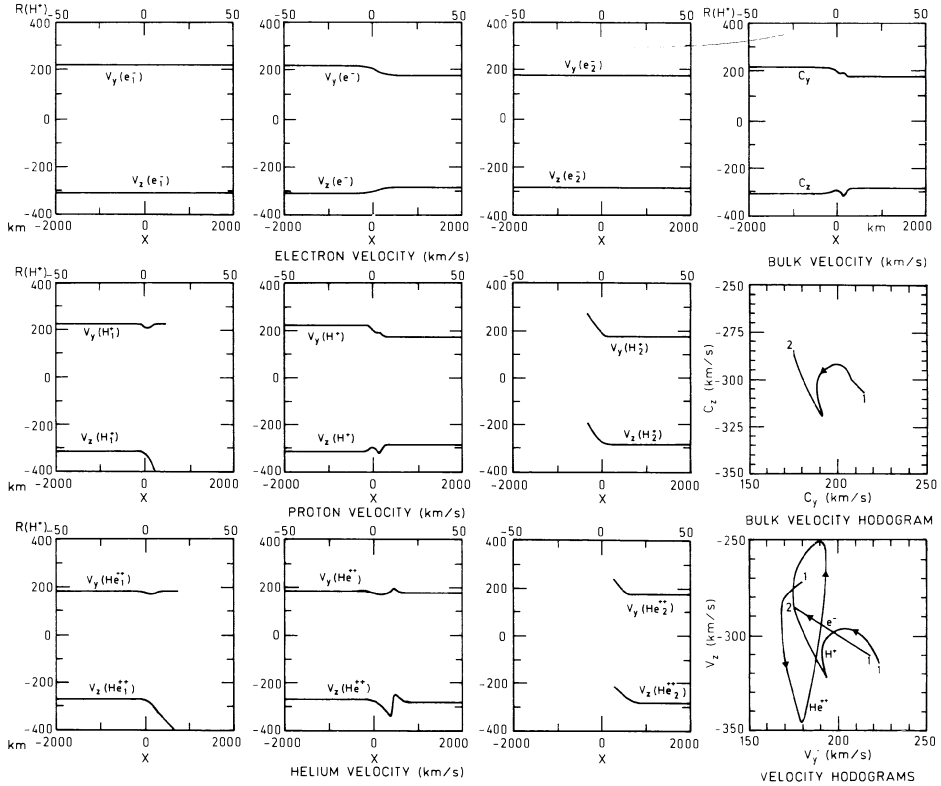


Figure 3. Flow characteristics across a TD whose boundary conditions are given in table I.

3. CONCLUSIONS

The results shown in this paper indicate how to model a tangential discontinuity in the solar wind. This modeling of current sheets is one aspect of the Interdisciplinary Study of Directional Discontinuities in the Solar Wind with the Ulysses Mission (Lemaire et al., 1983). One of the objective of this Interdisciplinary Study is a detailed comparison of theoretical calculations with magnetic-field and particle-flux measurements. As shown in this paper, the theoretical thickness for current sheets in the solar wind is expected to be of the order of $20 R(H^+)$ or less. The time resolution of present-day magnetic-field measurements in space is usually high enough to de-

termine the fine structure of such sharp magnetic-field "discontinuities", but the best time resolution for direct plasma measurements is generally much lower. A time of at least 10 s is required to sample particles in all energy ranges and in all velocity directions. Over such a long period, a spacecraft has travelled a distance of 4000 km in the frame of the supersonic solar wind plasma. Since the actual time resolution of solar wind plasma instruments will be much larger than the time (1-5 s) required for a interplanetary vehicle to pass through a thin current sheet, the particle fluxes measured in successive energy channels and successive solid angles must be compared directly with the corresponding values deduced from theoretical velocity distributions calculated at different depths in the current sheet.

REFERENCES

- ALPERS, W., 1969, *Astrophys. Space Sci.*, **5**, 425-437.
LEE, L.C. and J.R. KAN, 1979, *J. Geophys. Res.*, **84**, 6417-6426.
LEMAIRE, J., M. ROTH, M. SCHERER and M. SCHULZ, 1983, *ESA SP-1050*, 265-271.
ROTH, M., 1978, *J. Atmos. Terr. Phys.*, **40**, 323-329.
ROTH, M., 1979, *ESA-SP-148*, 295-309.
ROTH, M., 1980, *Aeronomica Acta A n° 221*, also in 1984, *Acad. R. Belg., Mém. Cl. Sci.*, Collection in 8e-2e série, **44**(7) 222 pp.
ROTH, M., 1983, pp. 139-147, in : W. Bötticher, H. Wenk and E. Schulz-Gulde (Eds.), *Proceedings of the XVI International Conference on Phenomena in Ionized Gases, Düsseldorf*.